NJC

Accepted Manuscript

This is an *Accepted Manuscript*, which has been through the Royal Society of Chemistry peer review process and has been accepted for publication.

Accepted Manuscripts are published online shortly after acceptance, before technical editing, formatting and proof reading. Using this free service, authors can make their results available to the community, in citable form, before we publish the edited article. We will replace this *Accepted Manuscript* with the edited and formatted *Advance Article* as soon as it is available.

You can find more information about *Accepted Manuscripts* in the Information for Authors.

Please note that technical editing may introduce minor changes to the text and/or graphics, which may alter content. The journal's standard Terms & Conditions and the Ethical guidelines still apply. In no event shall the Royal Society of Chemistry be held responsible for any errors or omissions in this *Accepted Manuscript* or any consequences arising from the use of any information it contains.

ROYAL SOCIETY OF CHEMISTRY

www.rsc.org/njc

Push-pull porphyrins with different anchoring group orientation for fully printable monolithic dye-sensitized solar cells with mesoscopic carbon counter electrodes

Jiangzhao Chen, Yusong Sheng, Songguk Ko, Linfeng Liu, Hongwei Han, Xiong Li*

Michael Grätzel Center for Mesoscopic Solar Cells, Wuhan National Laboratory for Optoelectronics, Huazhong University of Science and Technology, Wuhan 430074, Hubei, P. R. China

* Correspondence to: Xiong Li (Email address: lxwhu2008@hotmail.com)

Tel: +86 27 87793027; fax: +86 27 87793027

Abstract: Here, four D-π-A porphyrin dye molecules with carboxylic acid at para-position or meta-position of benzene ring (coded as **WH-C4**, **WH-C1**, **WH-C6** and **WH-C7**, respectively) were designed and synthesized for monolithic dye-sensitized solar cells with mesoscopic carbon counter electrodes. Significant optical and electrochemical differences were found for **WH-C6** and **WH-C7** with carboxylic acid at meta-position of benzene ring in comparison with **WH-C4**, **WH-C1** with carboxylic acid at para-position of benzene ring. The influence of anchoring group positions on the photovoltaic performance of corresponding devices was systematically investigated. The devices sensitized by **WH-C6** and **WH-C7** shows inferior open circuit voltage (V_{oc}) and short circuit photocurrent (J_{sc}) compared with that sensitized by **WH-C4** and **WH-C1**. The above performance differences were confirmed and explained by electrochemical impedance spectroscopy (EIS), UV-visible absorption spectra and dye loading measurement, respectively.

Keywords: Monolithic dye-sensitized solar cells; Push-pull porphyrins; Anchoring

group orientation; Carbon counter electrodes

1. Introduction

Dye-sensitized solar cells (DSSCs) are one of promising photovoltaic devices which can convert efficiently sunlight to electricity, attracting extensive attention because of their high power conversion efficiency(PCE), ease of fabrication and potential low cost compared with traditional silicon-based solar cells.[1-3] DSSCs is mainly composed of dye-sensitized nanocrystalline oxide, electrolytes and counter electrodes (CEs)，among which dyes as one of important components play a key role in determining the photovoltaic performance of the devices. In the past two decades, although optimized Rupolypyridyl sensitizers have achieved PCEs of over 11%[4-6] due to their broad absorption spectrum through metal-to-ligand charge transfer (MLCT), the longer exciton lifetime, and their long-term chemical stability,[7, 8] several drawbacks[8-10] such as the high cost of noble metal ruthenium, the requirement for careful synthesis, tricky purification steps and low molar extinction coefficient are obstacle of its large-scale application. Under such circumstances, it seems to be an effective solution to these problems to seek alternative sensitizers.

Among dyes under investigation, porphyrins as an alternative sensitizer for polypyridyl ruthenium dyes DSSCs have aroused widespread interest due to its low cost, high molar extinction coefficients and structural diversity.[11-13] Motivated by the above advantages, considerable efforts have been devoted to develop new and efficient porphyrin sensitizers. Before 2009, most porphyrin sensitizers were designed

through the connection of anchoring groups to the meso or β–position of porphyrin ring without additional electron-donating donors, leading to the low PCEs (generally <7%). Recent several years, as similar as the structures of the most organic dyes, the porphyrin dyes are also designed according to basic structures of Donor-π-conjugated bridge-Acceptor (simplified as D-π-A) which are beneficial to intramolecular electron transportation. Benefitted from the introduction of D-π-A push-pull structure, great progress has been made in the past few years.[13-16] Thereinto, through the cosensitization of the porphyrin **YD2-o-C8** with excellent organic dye **Y123** based on Cobalt (II/III) redox electrolyte, a record efficiency as high as 12.3% has been achieved by judicious molecular engineering methodology.[17] Subsequently, the DSSCs based on judiciously engineered push-pull porphyrin sensitizer **SM315**, which was obtained through inserting benzothiadiazole unit between porphyrin ring and benzoic acid accepter, achieved a world record liquid state efficiency of 13% using Cobalt (II/III) redox electrolyte.[18] Recently, the solar cell cosensitized by organic dye **C1** and the porphyrin **XW4** with an extended conjugation framework and a carbazole donor exhibited a high PCE of 10.45% with an improved current density (J_{sc}) and an open-circuit voltage (V_{oc}) values.[19] Additionally, push–pull Zn-porphyrin **WW-6** functionalized via N-annulated perylene as an efficient electron donor displayed a power conversion efficiency as high as 10.5% using Cobalt (II/III) redox electrolyte, which is comparable to that of the **YD2-o-C8** cell (η = 10.5%) under the same conditions.[20] The above experiment results adequately testify the importance of push–pull D-π-A Zn-porphyrin design. So in the present study, we design and

synthesize push–pull D-π-A Zn-porphyrin. Although very high PCEs have been achieved, there is still room for PCEs improvement through rational modification and engineering of porphyrin molecule structures. It is well known that the performance of porphyrin sensitized solar cells is limited by its serious aggregation. In order to alleviate the aggregation of D-π-A porphyrin dye molecule, here we explore the possibility of improving the photovoltaic performance of D-π-A porphyrin-sensitized solar cells by increasing the asymmetry induced via different anchoring group positions. Actually, it has been demonstrated previously that the acceptor in D-π-A structure is of great importance in determining the photovoltaic performance of DSSCs through influencing the photophysical and electrochemical properties of the sensitizers along with the function mode with TiO_2. Obviously, kinds of anchoring groups have significant effects on the binding mode of dyes on TiO_2. Actually, over past two decades, a variety of anchoring groups such as carboxylic acid groups, sulphonic acid groups,[21] phosphonic acid groups[22] and pyridine ring,[23] have been applied to various sensitizers for DSSCs. To explore the application of porphyrins as light-harvesting materials with various anchoring groups, Lu *et al.*[24] reported a dye **LW11** with pyridine ring as anchoring group for DSSCs. It was found that dye **LD14** with the conventional carboxylic acid as acceptor possessed much better photovoltaic performance than **LW11**. Nevertheless, to date, anchoring group the most widely and successfully used is still carboxylic acid. So in this study, we choose carboxylic acid as anchoring group in push–pull D-π-A porphyrin dyes.

In reality, except for the kinds of anchoring groups, positions of anchoring

groups in different dyes have important influence on the photovoltaic performance of DSSCs. But literature on the influence of anchoring group positions on the photovoltaic performance of DSSCs was very limited. Hart *et al.* [25] synthesized porphyrin **1m-Zn** and **1p-Zn** with carboxyl anchoring group incorporated at the meta or para-position of benzene ring, respectively, which have no additional strong electron-donating donor at the meso or β–position of porphyrin ring. It was found that **1m-Zn** exhibited higher J_{sc} and V_{oc} than **1p-Zn**. In order to improve further the performance of porphyrin sensitized solar cells, it is significantly meaningful to further investigate if anchoring group position change from para-position to meta-position of benzene ring in D-π-A structural porphyrin with additional different strong electron-donating donors at the meso–position of porphyrin ring sensitizers can improve the photovoltaic performance of DSSCs. Consequently, here we designed and synthesized two new push-pull porphyrin dye molecules with carboxylic acid at meta-position of benzene ring, coded as **WH-C6** with carbazole as donor and **WH-C7** with 4,4'-dimethyltriphenylamine as donor, respectively. Simultaneously, we also synthesized **WH-C1** and **WH-C4** with carboxylic acid at para-position of benzene ring for convenient comparison, which have been reported by our previous literatures.[26, 27] Accordingly, the influence of anchoring group positions on the photophysical and electrochemical characteristics of porphyrin sensitizers were systematically investigated. It was found that anchoring group positions significantly influence the HOMO, LUMO levels and molar absorption ability of porphyrin molecules. To further scrutinize the relationship between porphyrin sensitizers with

different anchoring group positions and the photovoltaic performance of DSSCs sensitized by the corresponding porphyrin dyes, a fully printable low-cost monolithic cell architecture with mesoscopic carbon counter electrodes was utilized to fabricate the complete DSSC devices. It was found that **WH-C4** and **WH-C1** with carboxylic acid at para-position of benzene ring shows much better photovoltaic performance than **WH-C6** and **WH-C7** with carboxylic acid at meta-position of benzene ring.

2. Experimental

2.1. Materials

All reagents and solvents were obtained from commercial sources and used without further purification unless otherwise noted. Solvents used for reactions were dried by standard procedures. All reactions were carried out under N_2 atmosphere. Column chromatography of all the products was performed on silica gel (Kanto, Silica Gel 60N, spherical, 200–300 mesh), and some were further purified by recrystallization.[5,15-Bis(2,6-di-octoxyphenyl)-10,20-Bis[(triisopropylsilyl)ethynyl]-porphinato] zinc(II)(**1**),[26, 27] 3-iodo-9-ethyl-9H-carbazole[27] and N,N-bis(4-methylphenyl)-N-(4-iodophenyl)[26] was synthesized as the previously reported method.

2.2. Preparation of platinized carbon paste

Platinized carbon paste was prepared as described elsewhere.[28] 2 g carbon black powders (particle size: 30 nm) and H_2PtCl_6 (Sigma) with a predetermined Pt/carbon black weight ratio were added into 20 ml isopropanol solution (Sigma) under continue stirring for 30 min, and then the paste was sintered for 30 min at 380 ◦C in furnace to

thermally deposit the Pt nanoparticles on the surface of carbon black, followed by mixing with graphite powders (particle size: 1.3 μm) with a predetermined graphite/carbon black weight ratio. Finally, 1 g of 20 nm ZrO_2 nanopowders (Sigma) and 1 g of hydroxypropyl cellulose (Sigma) were added into a 30 ml terpineol solution. The platinized carbon material paste was obtained after stirring vigorously using ball milling for 2 h.

2.3. Characterization

UV-visible spectra were performed on PerKinElmer Lambda 950 spectrophotometer. ^{1}H NMR and ^{13}C NMR spectra were recorded on Bruker-AV400 spectrometers with 400 MHz. The chemical shifts were recorded in parts per million (ppm) with TMS as the internal reference. ESI mass spectra were measured on Finnigan LCQ Advantage mass spectrometer. The cyclic voltammetrys (CVs) were carried out with a three-electrode system in an argon-purged electrolyte solution on PARSTAT 2273 Electrochemical Workstation. Cyclic voltammograms for porphyrin dyes were conducted with a three-electrode cell equipped with a BAS glassy carbon (0.07 cm^2) disk as the working electrode, a platinum wire as the auxiliary electrode, and a Ag/AgCl (saturated) reference electrode. The working electrode was polished with 0.03 μm alumina on felt pads (Buehler) and treated ultrasonically for 1 min before each experiment. The potential of the reference electrode was adjusted by recording the cyclic voltammogram for 0.01 M ferrocene in THF containing 0.1 M $TBAPF_6$. The thickness of all films was measured with a profilometer (VeecoDektak 150).

2.4. Device fabrication

A compact layer of TiO_2 was deposited on the FTO-coated glass by spray pyrolysis deposition with di-isopropoxytitanium bis(acetyl acetonate) solution. Subsequently a 8μm-thick mesoporous TiO_2 (particle size, 20 nm, PASOL HPW-18NR TiO_2 nanopowders, JGC Catalysts and Chemicals Ltd., Japan) transparent electrodes, a 3μm-thick spacer layer composed of 40 and 90-nm-sized zirconia particles, and a 50μm-thick mesoscopic platinized graphite/carbon black electrodes were prepared by screen printing onto FTO-coated conducting glass layer by layer, which were sintered at 500℃, 500℃ and 400℃ for 30min, respectively. Then the working electrode was prepared by immersing TiO_2 film into the 0.2mM dye solution (in Toluene/EtOH = 1/1,v/v) containing chenodeoxycholic acid (CDCA, 0.4 mM) at 25℃ overnight. The cell was encapsulated by a 100μm thick spacer of the thermo-bonding polymer (Surlyn, DuPont) with sheet glass. After sealing, the liquid electrolyte was injected into the cell through the hole predrilled in the sheet glass, and then the hole was sealed with Surlyn polymer and cover glass. The liquid electrolyte consisted of 1.0 M 1,2-dimethylimidazolium iodide (DMPII), 0.03M iodine, 0.1M guanidinium thiocyanate and 0.5M tert-butylpyridine in a mixture of acetonitrile/valeronitrile (85: 15, v/v).

2.5. Photovoltaic measurements

Current-voltage (*I-V*) characteristics were measured with a Keithley 2400 source/meter and a Newport solar simulator (model 91160) giving light with AM 1.5 G spectral distribution, which was calibrated using a certified reference solar cell

(Fraunhofer ISE) to an intensity 100 mW cm^{-2}. A black mask with a slightly smaller circular aperture (0.07 cm^2) than the active area of the square solar cell (0.25 cm^2) was applied on top of the cell. The incident photon-to-current conversion efficiency (IPCE) was measured using a 150W xenon lamp (Oriel) fitted with a monochromator (Cornerstone 260) as monochromatic light source. The illumination spot size was chosen to be slightly smaller than the active area of the DSSC test cells. IPCE photocurrents were recorded under short-circuit conditions using a Keithley 2400 source meter. The monochromatic photon flux was quantified by means of a calibrated silicon photodiode. Electrochemical impedance spectroscopy (EIS) of the symmetric cell was measured using PARSTAT 2273 Electrochemical Workstation in the frequency range 0.1 to 10^6 Hz with 10 mV AC amplitude. The complete DSSCs prepared under the same conditions were used to measure I-V, IPCE and EIS.

2.6. Synthesis

Synthesis of WH-C6

Compound **WH-C6** was prepared according to literature procedure.[29-31] To a solution of porphyrin **1** (98 mg, 0.07 mmol) in dry THF (20 mL) was added TBAF (1M in THF, 0.57 mL, 0.57 mmol). The solution was stirred at room temperature for 0.5 h. The mixture was concentrated and then extracted with CH_2Cl_2/H_2O. The organic layer was dried over anhydrous $MgSO_4$ and the solvent was removed under vacuum. The residue, 3-iodo-9-ethyl-9H-carbazole (25mg, 0.077mmol, 1.1eq), and 3-iodobenzoic acid (17 mg, 0.07mmol, 1.0eq) were dissolved in a mixture of THF (20 mL) and Et_3N (4 mL) and degassed with N_2 for 10 min, and then $Pd_2(dba)_3$ (33 mg, 0.036 mmol)

and $AsPh_3$ (88 mg, 0.29mmol) were added to the mixture. The solution was refluxed for 5 h under N_2 and the solvent was removed under reduced pressure. The residue was purified on a column chromatography (silica gel) using CH_2Cl_2/CH_3OH = 20/1 as eluent. Recrystallization from CH_2Cl_2/EtOH gave a green solid (34.3mg, 35%). ^{1}H NMR ($CDCl_3$/pyridine-d5, 600 MHz) δ_H 9.71 (d, *J* = 4.0 Hz, 2H), 9.63 (d, *J* = 4.0 Hz, 2H), 8.86 (t, *J* = 4.0 Hz, 4H), 8.75 (s, 1H), 8.71 (s, 1H), 8.51 (s, 1H), 8.24 (d, *J* = 7.5 Hz, 1H), 8.21 (d, *J* = 7.5 Hz, 1H), 8.12 (d, *J* = 7.3 Hz, 1H), 8.08 (d, *J* = 8.0 Hz, 1H), 7.72 (t, *J* = 8.5 Hz, 2H), 7.60 (t, *J* = 7.6 Hz, 1H), 7.53 (t, *J* = 8.3 Hz, 2H), 7.46 (d, *J* = 7.9 Hz, 1H), 7.04 (d, *J* = 8.5 Hz, 4H), 4.43 (q, *J* = 7.1 Hz, 2H), 3.88 (t, *J* = 5.9 Hz, 8H), 1.48 (t, *J* = 7.0 Hz, 3H), 1.23–1.10 (m, 8H), 0.99–0.85 (m, 8H), 0.79–0.70 (m, 8H), 0.66–0.55(m, 28H), 0.51-0.43 (m, 8H). ^{13}C NMR ($CDCl_3$/pyridine-d_5, 600 MHz) δ_C 168.9, 160.0, 151.6, 151.3, 150.5, 150.4, 140.4, 139.5, 134.9, 132.6, 132.4, 131.7, 131.4, 130.4, 130.2, 129.6, 129.3, 129.0, 128.5, 126.1, 125.0, 123.7, 123.4, 122.7, 121.4, 120.7, 119.3, 114.8, 108.7, 105.1, 101.0, 98.6, 96.8, 94.7, 94.2, 91.9, 68.5, 67.9, 67.0, 45.8, 37.7, 31.4, 28.8, 28.7, 28.6, 25.3, 22.3, 13.9. ESI-MS: m/z calcd for $C_{89}H_{99}N_5O_6Zn$: 1400; found 1400 $[M]^+$.

Synthesis of WH-C7

Compound **WH-C7** was synthesized from N,N-bis(4-methylphenyl)-N-(4-iodophenyl) amine (31mg, 0.077 mmol, 1.1eq) and 3-iodobenzoic acid (17 mg, 0.07mmol, 1.0eq) according to the synthetic procedure of **WH-C6**, giving a green solid (37.1 mg, 35.9%). ^{1}H NMR ($CDCl_3$/pyridine-d5, 600 MHz) δ_H 9.62 (d, *J* = 4.3 Hz, 2H), 9.57 (d, *J* = 4.3 Hz, 1H), 8.82 (d, *J* = 4.4 Hz, 2H),

8.80 (d, *J* = 4.4 Hz, 1H), 8.72 (s, 1H), 8.18 (d, *J* = 7.5 Hz, 1H), 8.05 (d, *J* = 7.3 Hz, 1H), 7.76 (d, *J* = 8.5 Hz, 2H), 7.72 (d, *J* = 6.5 Hz, 2H), 7.69 (d, *J* = 8.5 Hz, 2H), 7.56 (t, *J* = 7.4 Hz, 2H), 7.50 (t, *J* = 7.2 Hz, 1H), 7.13 (d, *J* = 8.4 Hz, 4H), 7.10 (d, *J* = 6.8 Hz, 4H), 7.02 (d, *J* = 8.6 Hz, 4H), 3.86 (t, *J* = 6.0 Hz, 8H), 2.34 (s, 6H), 1.02–0.94 (m, 8H), 0.94–0.86 (m, 8H), 0.80–0.70 (m, 8H), 0.66–0.53 (m, 28H), 0.50–0.41 (m, 8H). ^{13}C NMR ($CDCl_3$/pyridine-d_5, 600 MHz) δ_C 159.9, 151.6, 151.3, 150.4, 148.0, 144.8, 134.0, 133.1, 132.5, 132.2, 132.1, 131.6, 131.4, 131.3, 130.3, 130.0, 129.6, 129.3, 128.2, 125.1, 121.5, 121.3, 116.8, 114.8, 105.1, 100.5, 99.1, 95.7, 94.7, 94.1, 92.9, 68.5, 31.4, 28.8, 28.7, 28.6, 25.3, 22.3, 20.8, 13.9. ESI-MS: m/z calcd for $C_{95}H_{105}N_5O_6Zn$: 1478; found 1478 $[M]^+$.

3. Results and Discussion

3.1. Synthesis

In the present work, two novel porphyrin dyes with carboxylic acid anchoring group at meta-position of benzene ring (carbazole and 4,4'-dimethyltriphenylamine as donors at the meso-position opposite to the anchoring benzoic acid group) were designed and synthesized for monolithic DSSCs based on carbon/graphite counter electrodes,[28] coded as **WH-C6** and **WH-C7**, respectively. The structures of dyes and the synthetic route are shown in Fig. 1 and Scheme 1, respectively. The detailed synthetic procedures are presented in the experimental section. The molecular structures of target porphyrins were confirmed by ^{1}H NMR, ^{13}C NMR, ESI-MS, which are also given in the experimental section.

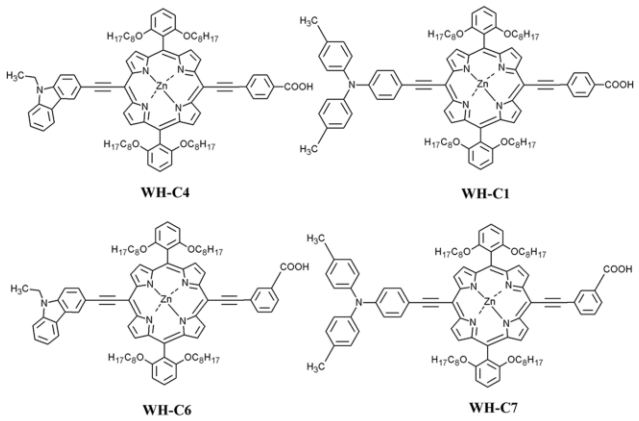

Fig. 1 Molecular structures of sensitizers in this study.

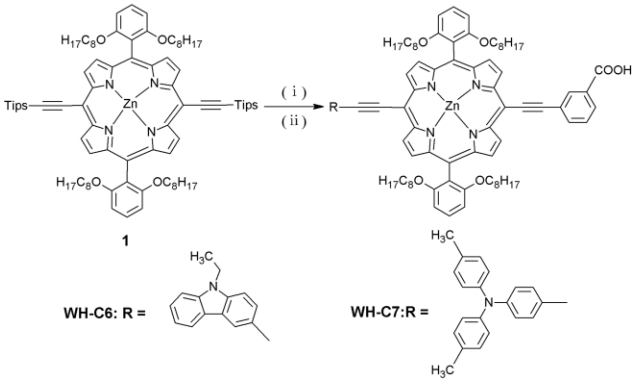

Scheme 1. Synthetic route of **WH-C6** and **WH-C7**. Reaction conditions: (ⅰ) TBAF in THF, THF, RT, 0.5h; (ⅱ) 3-iodo-9-ethyl-9H-carbazole or N,N-bis(4-methylphenyl)-N-(4-iodophenyl) amine, 3-iodobenzoic acid, $Pd_2(dba)_3$, $AsPh_3$, triethylamine, THF, 65℃, 5-8h.

3.2. Optical properties

The UV-vis absorption spectra of **WH-C4**, **WH-C1**, **WH-C6** and **WH-C7** in THF solution were depicted in Fig. 2. The corresponding peak positions and molar absorption coefficients (ε) of Soret and Q bands were listed in Table 1. As shown in Fig. 2**,** the four sensitizers exhibit typical porphyrin absorption characteristics with a strong Soret band appearing in the range of 400-500nm and mild Q bands appearing in the longer wavelength range of 600-700nm, which is attributed to π-π* charge

transfer transitions of the conjugated molecule and intramolecular charge transfer (ICT) transitions of the D-π-A conjugated backbone.[32] According to the absorption data in Table 1, it is observed obviously that Soret band and Q band peak positions for **WH-C6** and **WH-C7** are blue-shifted in comparison with **WH-C4** and **WH-C1**, respectively, which may be ascribed to inferior intramolecular charge transfer (ICT) of **WH-C6** and **WH-C7** compared with **WH-C4** and **WH-C1**. Apparently, the maximum molar extinction coefficients of Soret band of **WH-C6** and **WH-C7** are lower than that of **WH-C4** and **WH-C1**. Meanwhile, Fig. 3 presents the UV-visible absorption spectra of the sensitizers adsorbed on TiO_2 films. In comparison with absorption spectra in solution, the trend of the Soret and Q bands absorption spectra is similar when the sensitizers are adsorbed on TiO_2 films. Nevertheless, the Soret and Q absorption bands are broadened and corresponding absorption onsets are red-shifted conspicuously (seen in Figure 2 and 3). Thereinto, broadening of Soret and Q absorption bands is ascribed to the interaction between the dyes and TiO_2.[33, 34] Besides, the absorption of dyes on TiO_2 electrode is correlated with the aggregation morphology such as H-type or J-type aggregation. H-aggregates where molecules are aligned parallel to each other with strong intermolecular interaction tend to induce the nonradiative deactivation process.[35] Formation of H-aggregates is characterized by blue-shifted absorption bands with respect to those of the isolated chromophore. In contrast, J-aggregates where the molecules are arranged in head-to-tail direction induce a relatively high fluorescence efficiency with a bathochromic shift of UV absorption maximum.[35] Consequently, the red shift of absorption onsets is thought to

result from the formation of *J*-aggregates on TiO_2 electrode.[34] Additionally, the fluorescent emission spectra were measured in THF and shown in Fig. 4. For the fluorescence spectra, major emission bands are observed at 673, 674, 668 and 671 nm for **WH-C4**, **WH-C1**, **WH-C6** and **WH-C7**, respectively, which are similar to the trend of the Soret and Q bands absorption spectra. Consequently, it can be concluded that porphyrin dye molecules with carboxylic acid as anchoring group at meta-position of benzene ring possess significantly different optical properties compared with that of carboxylic acid as anchoring group at para-position of benzene ring.

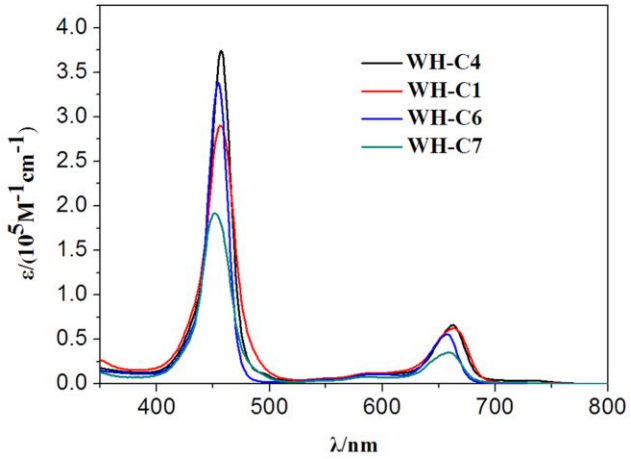

Fig. 2 UV-visible absorption spectra of sensitizers inTHF solvent.

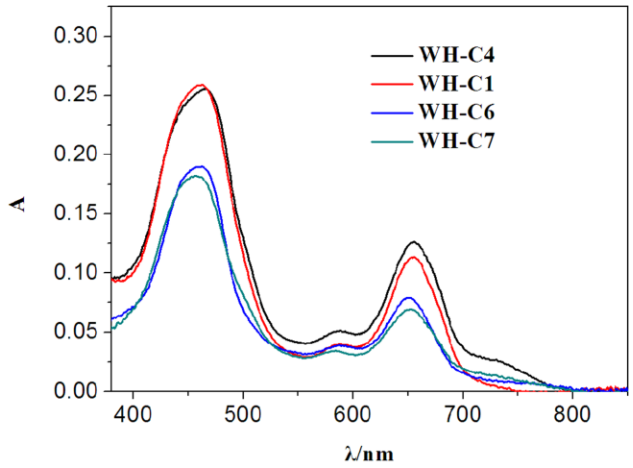

Fig. 3 UV-visible absorption spectra of the sensitizers adsorbed on TiO_2 films.

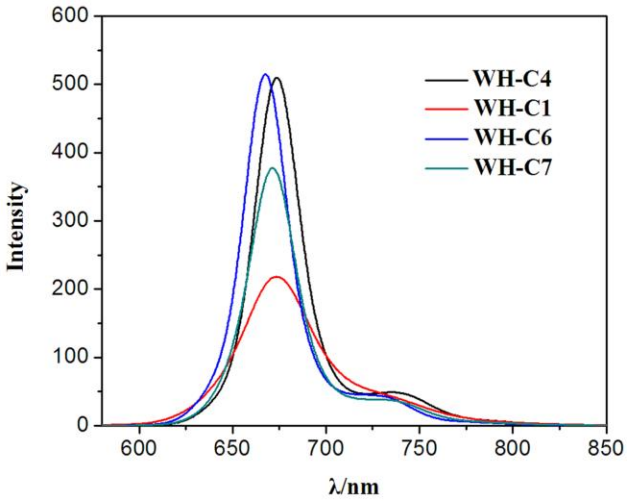

Fig. 4 Emission spectra of sensitizers in THF solvent.

Table 1 Photophysical and electrochemical properties of the sensitizers.

Dye	λ_{max}[a] /nm ($\varepsilon/10^4 M^{-1}cm^{-1}$)	Emission [a]λ_{max} /nm	E_{ox}[b]/V(vs. NHE)	$E_{0\text{-}0}$[c] /V(vs. NHE)	E_{LUMO}[d]/V(vs. NHE)	Dye loading[e]/10^{-7} $molcm^{-2}$
WH-C4	457(37.09),663(6.25)	673	0.861	1.944	-1.083	0.37
WH-C1	457(28.76),664(6.00)	674	0.860	2.016	-1.156	0.35
WH-C6	455(33.34),658(5.05)	668	0.849	1.985	-1.136	0.34
WH-C7	452(18.68),659(3.04)	671	0.837	1.949	-1.112	0.34

[a] Absorption and emission data were measured in THF at 25℃. Excitation wavelengths: 457 nm (**WH-C4**), 457 nm (**WH-C1**), 455 nm (**WH-C6**), 452nm (**WH-C7**). [b] The first porphyrin-ring oxidation was performed at 25℃ with each porphyrin (0.5 mM) in THF containing $TBAPF_6$(0.1M) under N_2 condition with a GC working electrode, a Pt counter electrode, and a Ag/AgCl reference electrode with a scan rate of 50 mV s^{-1}. [c] E_{0-0} was estimated from the intersection wavelengths of the normalized UV/Vis absorption and fluorescence spectra. [d] $E_{LUMO} = E_{ox} - E_{0\text{-}0}$. [e] the

amount of porphyrin dyes were carried out through the desorption of a 5 um TiO_2 film sensitized by dye in the 0.05 M solution of NaOH in THF/EtOH/H_2O(v/v/v, 1:1:1) for 2 days.

3.3. Electrochemical properties

In order to investigate the feasibility of electron injection and dye regeneration processes in DSSCs, Cyclic voltammetry measurements for the four dyes were performed in water-free THF containing 0.1 M tetrabutylammonium hexafluorophosphate ($TBAPF_6$) as the supporting electrolyte at room temperature and cyclic voltammograms are presented in Fig. 5. It is observed that electrochemical data for four dyes display quasi-reversible couples. The highest-occupied molecular orbitals (HOMOs) of dyes corresponding to the first redox potential were calculated to be 0.861, 0.860, 0.849 and 0.837V for **WH-C4**, **WH-C1**, **WH-C6** and **WH-C7**, respectively. Practically, it was confirmed that η_{inj} with unit efficiency requires approximately 0.2 V of over-potential ($-\Delta G$) between the TiO_2 conduction band (CB) and lowest unoccupied molecular orbital (LUMO) level of dye, and 0.3 V of $-\Delta G$ between the dye highest occupied molecular orbital (HOMO) level and redox potential for sufficient driving forces of electron injection from the dye to the CB of TiO_2 and the regeneration of oxidized dye.[36, 37] It is observed that the HOMO levels of four porphyrin dyes are sufficiently more positive than the iodine/iodide redox potential value (0.4 V vs. NHE),[38] guaranteeing the efficient regeneration of oxidized dye through I^- present in the electrolyte of the DSSCs. The zero–zero excitation energies (E_{0-0}) were calculated to be 1.944 V (**WH-C4**), 2.016 V (**WH-C1**), 1.985 V

(**WH-C6**) and 1.949 V (**WH-C7**) by the intersection of the normalized UV-vis absorption spectrum and steady-state fluorescence emission spectrum. The lowest-unoccupied molecular orbitals (LUMOs) levels of all porphyrin sensitizers were determined according to the expression of LUMO = HOMO - $E_{0\text{-}0}$ and corresponding level values were summarized in Table 1. Obviously, the LUMO levels of all dyes are sufficiently more negative compared with the conduction band edge level (E_{cb}) of the TiO_2 electrode (-0.5 V vs. NHE), which means that electron injection from the excited dye into the conduction band of TiO_2 is thermodynamically feasible. Therefore, these dyes are appropriately used as sensitizers for DSSCs.

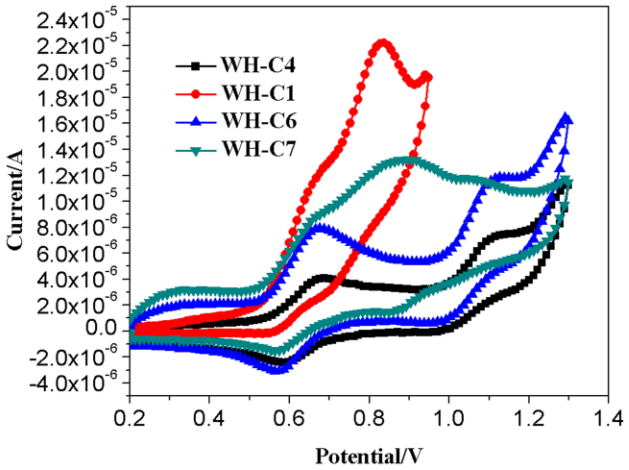

Fig. 5 Cyclic voltammograms of sensitizers in THF at a scan rate of 50 mV/s at room temperature with 0.1 M tetra-n-butylammonium hexafluorophosphate($TBAPF_6$) as the supporting electrolyte. GC working electrode, Pt wire counter electrode, and Ag/AgCl reference electrode were used.

3.4. Photovoltaic performance of DSSCs

Monochromatic incident photo-to-current conversion efficiency (IPCE) for DSSCs is mainly determined by the light harvesting efficiency (η_{LHE}), the electron

injection yield (η_{inj}) and the charge collection efficiency (η_{cc}).[36, 39] Among them, η_{LHE} and η_{inj} being closely related to dye contribute to improvement of IPCE greatly. In the past, it was demonstrated that the molecular structures of sensitizers have a significant influence on η_{LHE} and η_{inj} through influencing their Photophysical and electrochemical properties. In this work, we synthesized two novel push-pull porphyrin dye molecules with carboxylic acid at meta-position of benzene ring, coded as **WH-C6** with carbazole as donor and **WH-C7** with 4,4'-dimethyltriphenylamine as donor, respectively. For convenient comparison, we also synthesized **WH-C1** and **WH-C4** with carboxylic acid at para-position of benzene ring. The IPCEs for DSSCs based on the four dyes are presented in Fig. 6. As shown in Fig. 6, it is observed obviously that two peaks are located in the range of 400-500nm and 600-700nm, respectively, which is in agreement with UV-visible absorption spectra of the dyes. Besides, it is found that **WH-C6** and **WH-C7** possess lower IPCEs values at Soret and Q absorption bands than **WH-C4** and **WH-C1**, which is consistent with the trends of corresponding Soret and Q absorption bands. Compared with **WH-C1** and **WH-C7** with 4,4'-dimethyltriphenylamine as donor, **WH-C4** and **WH-C6** with carbazole as donor show lower IPCEs values, which is opposite to the trends of corresponding Soret and Q absorption bands. The phenomenon could be explained by more serious recombination reaction between the electron injected into the conduction band of TiO_2 and I_3^- at the vicinity of TiO_2 for **WH-C4** and **WH-C6**. In fact, we previously reported that **WH-C5** with triphenylamine as donor shows higher IPCE than **WH-C4** with carbazole as donor because of enhanced electron lifetimes.[27] Now η_{cc} competes

with η_{LHE}. In a word, although **WH-C4** and **WH-C6** have higher η_{LHE} than **WH-C1** and **WH-C7**, **WH-C1** and **WH-C7** show higher IPCE and J_{sc} because of their significantly enhanced electron lifetime than **WH-C4** and **WH-C6**, which is in good agreement with previous report.[27]

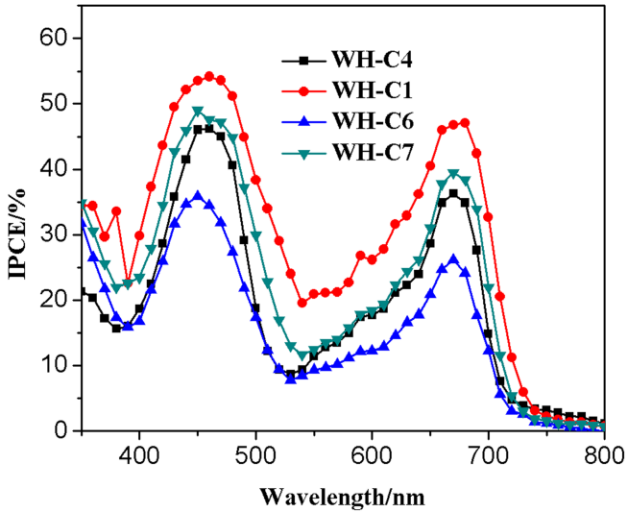

Fig. 6 Monochromatic incident photon-to-current conversion efficiency (IPCE) action spectra for DSSCs based on **WH-C4**, **WH-C1**, **WH-C6** and **WH-C7**.

The current density-voltage (I-V) curves of the DSSCs sensitized by **WH-C4**, **WH-C1**, **WH-C6** and **WH-C7** are displayed in Fig. 7 with corresponding detailed photovoltaic performance parameters listed in Table 2. Under standard global air mass 1.5 solar conditions, **WH-C4** and **WH-C1** sensitized cells gave a short circuit photocurrent density (J_{sc}) of 10.07 and 12.18 mA cm^{-2}, an open circuit voltage (V_{oc}) of 609.81 and 639.48 mV, and a fill factor (*FF*) of 0.72 and 0.72, corresponding to an overall conversion efficiency (η) of 4.40% and 5.58%, respectively. Under the same conditions, **WH-C6** and **WH-C7** sensitized cells exhibited a J_{sc} of 8.53 and 9.81 mA cm^{-2}, a V_{oc} of 599.44 and 604.25 mV, and a *FF* of 0.73 and 0.73, corresponding to a η

of 3.75% and 4.30%, respectively. Compared with **WH-C4** and **WH-C1**, the cells based on **WH-C6** and **WH-C7** show inferior J_{sc} and V_{oc}. In order to explain the above difference, we performed dye loading measurement through adsorbing the dyes onto TiO_2 films. The loading amount of **WH-C4**, **WH-C1**, **WH-C6** and **WH-C7** was calculated to be 0.37×10^{-7}, 0.35×10^{-7}, 0.34×10^{-7} and 0.34×10^{-7} mol • cm^{-2}, respectively. Consequently, the lower J_{sc} of **WH-C6** and **WH-C7** could be attributed to the lower dye loading amount. Furthermore, the carboxyl anchoring group of **WH-C6** and **WH-C7** located at the meta-position of benzene ring could be detrimental to intramolecular charge transfer and eventually influenced electron injection efficiency, which resulted in low IPCE and short circuit current. As we all know, there are two kinds of recombination reactions in DSSCs. First, the oxidized dye can recombine with the electrons injected into the conduction band of TiO_2. Second, I_3^- in electrolyte can also recombine with the electrons injected into the conduction band of TiO_2. Although Hart *et al.*[25] reported that porphyrin **1m-Zn** with carboxyl anchoring group incorporated at the meta-position of benzene ring shew higher J_{sc} and V_{oc} in comparison with **1p-Zn** with carboxyl anchoring group incorporated at the para-position of benzene ring, which be ascribed to the lower dye absorbing amount of **1p-Zn** and inhibition of the above second recombination reaction. However, here we draw opposite conclusions in D-π-A porphyrin. Carboxyl anchoring group introduced at the meta-position of benzene ring not only reduces the dye loading amount because of steric hindrance but also could accelerate the above two recombination reaction, leading to lower J_{sc} and V_{oc} of **WH-C6** and **WH-C7**

relative to **WH-C4** and **WH-C1**.

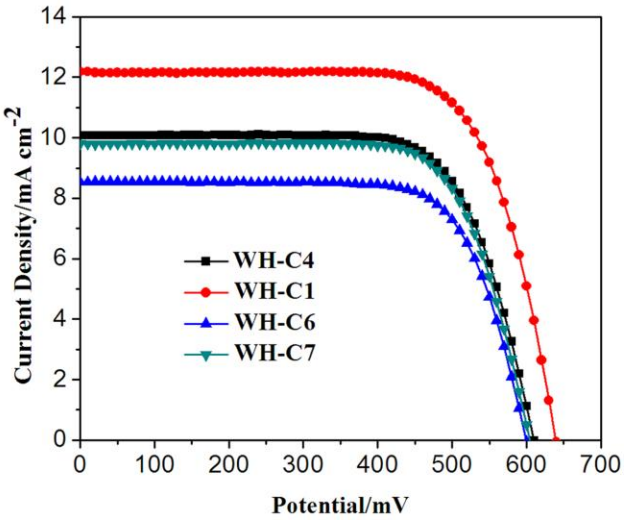

Fig. 7 Current-voltage characteristics of DSSCs sensitized with **WH-C4**, **WH-C1**, **WH-C6** and **WH-C7** under AM 1.5G simulated solar light (100 mW cm^{-2}).

Table 2 The photovoltaic performance parameters[a] of the DSSCs employing **WH-C4**, **WH-C1**, **WH-C6** and **WH-C7** under AM 1.5G simulated solar light (100 mW cm^{-2}).

Dye	V_{oc}/mV	J_{sc}/mA cm^{-2}	*FF*	η/%
WH-C4	609.81±10	10.07±0.03	0.72±0.01	4.40±0.01
WH-C1	639.48±10	12.18±0.10	0.72±0.01	5.58±0.04
WH-C6	599.44±10	8.53±0.04	0.73±0.00	3.75±0.02
WH-C7	604.25±8	9.81±0.20	0.73±0.01	4.30±0.10

[a] The photovoltaic parameters are averaged values obtained from analysis of the *J-V* curves of three identical devices fabricated and characterized under the same experimental conditions for each dye. The uncertainties represent two standard deviations of the measurements.

3.5. Electrochemical impedance spectroscopy (EIS)

To further investigate and elucidate the photovoltaic results and gain a better insight into the interfacial charge transfer process of the DSSCs with the different dyes, we performed electrochemical impedance spectroscopy measurements in the dark under a forward bias of -0.6V. The Nyquist plots for the devices based on **WH-C4**, **WH-C1, WH-C6** and **WH-C7** are shown in Fig. 8. As shown in Fig. 8, the first semicircle is assigned to impedances related to charge transport at the electrolyte/counter electrode interface. In the middle frequency range, the large semicircle is ascribed to the electron recombination resistance (R_{rec}) and chemical capacitance at the working electrode /electrolyte.[40, 41] It is obvious that the semicircle resulting from R_{rec} based on different dyes is in the order of **WH-C6** < **WH-C7** < **WH-C4** < **WH-C1**, indicating that the electron recombination resistance is also in the same order of **WH-C6** < **WH-C7** < **WH-C4** < **WH-C1**.[36] As shown in Fig. 7, the order of open circuit voltages for **WH-C6**, **WH-C7**, **WH-C4** and **WH-C1** is in agreement with the order of the electron recombination resistance. EIS results suggest that carboxylic acid anchoring group orientation can influence the electron lifetimes via affecting the recombination reactions between the electrons injected into the conduction band of TiO_2 and the oxidized dye or I_3^- in electrolyte.

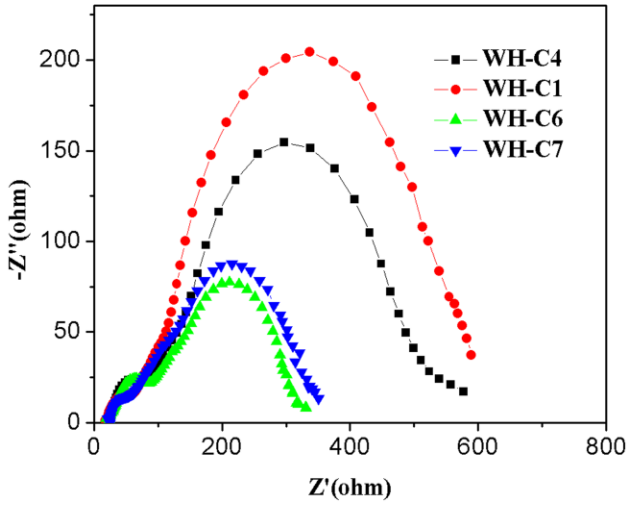

Fig. 8 Electrochemical impedance spectroscopy (Nyquist plots) for DSSCs based on **WH-C4**, **WH-C1**, **WH-C6** and **WH-C7** in the dark under a forward bias of -0.6 V.

4. Conclusions

In summary, we designed and synthesized two novel push-pull porphyrin dye molecules (**WH-C6** and **WH-C7**) with carboxylic acid anchoring group at meta-position of benzene ring for monolithic dye-sensitized solar cells. Simultaneously, we also synthesized previously reported porphyrin dyes (**WH-C4** and **WH-C1**) with carboxylic acid anchoring group at para-position of benzene ring for convenient comparison. We investigate systematically the effect of anchoring group position orientation on the photovoltaic performance of monolithic donor-π-conjugated bridge-acceptor (simplified as D-π-A) porphyrin-sensitized solar cells based on mesoscopic carbon counter electrodes. Compared with **WH-C4** and **WH-C1**, **WH-C6** and **WH-C7**-sensitized solar cells show inferior photovoltaic performance. Herein, it is demonstrated that the introduction of carboxylic acid anchoring group at meta-position of benzene ring in push-pull porphyrin dye molecules (seen in Fig. 1) not only reduces the dye loading amount because of steric

hindrance but also could accelerate electron recombination back reaction. The performance difference caused by anchoring group positions indicates that the structures of dye molecules are related closely to the performance of the device. The investigation offers directions for the rational design of high performance push-pull porphyrin dye molecules. In order to achieve highly efficient porphyrin-sensitized solar cells, elaborate design of donor, π-conjugated spacer and acceptor is indispensable.

Acknowledgments

The authors acknowledge the financial support by the Ministry of Science and Technology of China (863, No. SS2013AA50303), the National Natural Science Foundation of China (Grant No. 61106056), the fundamental Research Funds for the Central Universities (HUSTNY022), and Scientific Research Foundation for Returned Scholars, Ministry of Education of China. We also thank the Analytical and Testing Center of Huazhong University of Science and Technology [HUST] for NMR, MS, UV-vis absorption and emission spectra measurements.

Reference

1 B. O'Regan and M. Gratzel, *Nature*, 1991, **353**, 737.

2 A. Hagfeldt, G. Boschloo, L. Sun, L. Kloo and H. Pettersson, *Chem. Rev.*, 2010, **110**, 6595.

3 B. E. Hardin, H. J. Snaith and M. D. McGehee, *Nat. Photonics*, 2012, **6**, 162.

4 M. K. Nazeeruddin, F. De Angelis, S. Fantacci, A. Selloni, G. Viscardi, P. Liska, S. Ito, B. Takeru and M. Grätzel, *J. Am. Chem. Soc.*, 2005, **127**, 16835.

5 F. Gao, Y. Wang, D. Shi, J. Zhang, M. Wang, X. Jing, R. Humphry-Baker, P. Wang, S. M.

Zakeeruddin and M. Grätzel, *J. Am. Chem. Soc.*, 2008, **130**, 10720.

6 L. Han, A. Islam, H. Chen, C. Malapaka, B. Chiranjeevi, S. Zhang, X. Yang and M. Yanagida, *Energy Environ. Sci.*, 2012, **5**, 6057.

7 B. G. Kim, K. Chung and J. Kim, *Chem.-Eur. J.*, 2013, **19**, 5220.

8 C. W. Lee, H. P. Lu, C. M. Lan, Y. L. Huang, Y. R. Liang, W. N. Yen, Y. C. Liu, Y. S. Lin, E. W. G. Diau and C. Y. Yeh, *Chem.-Eur. J.*, 2009, **15**, 1403.

9 W. Zhou, B. Zhao, P. Shen, S. Jiang, H. Huang, L. Deng and S. Tan, *Dyes Pigments*, 2011, **91**, 404.

10 C.-Y. Lin, C.-F. Lo, L. Luo, H.-P. Lu, C.-S. Hung and E. W.-G. Diau, *J. Phys. Chem. C*, 2008, **113**, 755.

11 J. K. Park, J. Chen, H. R. Lee, S. W. Park, H. Shinokubo, A. Osuka and D. Kim, *J. Phys. Chem. C*, 2009, **113**, 21956.

12 M. V. Martínez-Díaz, G. de la Torre and T. Torres, *Chem. Commun.*, 2010, **46**, 7090.

13 L.-L. Li and E. W.-G. Diau, *Chem. Soc. Rev.*, 2013, **42**, 291.

14 M. Urbani, M. Grätzel, M. K. Nazeeruddin and T. s. Torres, *Chem. Rev.*, 2014, **114**, 12330.

15 Y. Wang, X. Li, B. Liu, W. Wu, W. Zhu and Y. Xie, *RSC Adv.*, 2013, **3**, 14780.

16 B. Liu, W. Zhu, Y. Wang, W. Wu, X. Li, B. Chen, Y.-T. Long and Y. Xie, *J. Mater. Chem.*, 2012, **22**, 7434.

17 A. Yella, H.-W. Lee, H. N. Tsao, C. Yi, A. K. Chandiran, M. K. Nazeeruddin, E. W.-G. Diau, C.-Y. Yeh, S. M. Zakeeruddin and M. Grätzel, *Science*, 2011, **334**, 629.

18 S. Mathew, A. Yella, P. Gao, R. Humphry-Baker, B. F. Curchod, N. Ashari-Astani, I. Tavernelli, U. Rothlisberger, M. K. Nazeeruddin and M. Grätzel, *Nat. Chem.*, 2014, **6**, 24.

19 Y. Wang, B. Chen, W. Wu, X. Li, W. Zhu, H. Tian and Y. Xie, *Angew. Chem., Int. Ed.*, 2014, **53**,

10779.

20 J. Luo, M. Xu, R. Li, K.-W. Huang, C. Jiang, Q. Qi, W. Zeng, J. Zhang, C. Chi, P. Wang and J. Wu, *J. Am. Chem. Soc.*, 2013, **136**, 265.

21 R. Ali, H. Naz and S. Shah, *Dyes Pigments*, 2013, **99**, 571.

22 I. López‐Duarte, M. Wang, R. Humphry‐Baker, M. Ince, M. Martínez‐Díaz, M. K. Nazeeruddin, T. Torres and M. Grätzel, *Angewandte Chemie*, 2012, **124**, 1931.

23 L. Wang, X. Yang, S. Li, M. Cheng and L. Sun, *RSC Adv.*, 2013, **3**, 13677.

24 J. Lu, X. Xu, Z. Li, K. Cao, J. Cui, Y. Zhang, Y. Shen, Y. Li, J. Zhu and S. Dai, *Chem.-an Asian. J.*, 2013, **8**, 956.

25 A. S. Hart, C. B. KC, H. B. Gobeze, L. R. Sequeira and F. D'Souza, *ACS Appl. Mater. Interface*, 2013, **5**, 5314.

26 J. Chen, S. Ko, L. Liu, Y. Sheng, H. Han and X. Li, *New Journal of Chemistry*, 2015, DOI: 10.1039/c4nj02186j.

27 J. Chen, S. Ko, L. Liu, Y. Sheng, H. Han and X. Li, *New Journal of Chemistry*, 2015, DOI: 10.1039/c4nj02263g.

28 G. Liu, H. Wang, X. Li, Y. Rong, Z. Ku, M. Xu, L. Liu, M. Hu, Y. Yang and P. Xiang, *Electrochimica Acta*, 2012, **69**, 334.

29 C.-P. Hsieh, H.-P. Lu, C.-L. Chiu, C.-W. Lee, S.-H. Chuang, C.-L. Mai, W.-N. Yen, S.-J. Hsu, E. W.-G Diau and C.-Y. Yeh, *J. Mater. Chem.*, 2010, **20**, 1127.

30 S.-L. Wu, H.-P. Lu, H.-T. Yu, S.-H. Chuang, C.-L. Chiu, C.-W. Lee, E. W.-G. Diau and C.-Y. Yeh, *Energy Environ. Sci.e*, 2010, **3**, 949.

31 T. Ripolles-Sanchis, B.-C. Guo, H.-P. Wu, T.-Y. Pan, H.-W. Lee, S. R. Raga, F. Fabregat-Santiago, J.

Bisquert, C.-Y. Yeh and E. W.-G Diau, *Chem. Commun.*, 2012, **48**, 4368.

32 H. Imahori, T. Umeyama and S. Ito, *Acc. Chem. Res.*, 2009, **42**, 1809.

33 K. Hara, M. Kurashige, Y. Dan-oh, C. Kasada, A. Shinpo, S. Suga, K. Sayama and H. Arakawa, *New J. Chem.*, 2003, **27**, 783.

34 J.-J. Kim, H. Choi, J.-W. Lee, M.-S. Kang, K. Song, S. O. Kang and J. Ko, *J. Mater. Chem.*, 2008, **18**, 5223.

35 B.-K. An, S.-K. Kwon, S.-D. Jung and S. Y. Park, *J. Am. Chem. Soc.*, 2002, **124**, 14410.

36 S. Zhang, X. Yang, Y. Numata and L. Han, *Energy Environ. Sci.*, 2013, **6**, 1443.

37 T. Daeneke, A. J. Mozer, Y. Uemura, S. Makuta, M. Fekete, Y. Tachibana, N. Koumura, U. Bach and L. Spiccia, *J. Am. Chem. Soc.*, 2012, **134**, 16925.

38 M. Wang, C. Grätzel, S. M. Zakeeruddin and M. Grätzel, *Energy Environ. Sci.*, 2012, **5**, 9394.

39 M. K. Nazeeruddin, A. Kay, I. Rodicio, R. Humphry-Baker, E. Müller, P. Liska, N. Vlachopoulos and M. Grätzel, *J. Am. Chem. Soc.*, 1993, **115**, 6382.

40 L. Han, N. Koide, Y. Chiba and T. Mitate, *Appl. Phys. Lett.*, 2004, **84**, 2433.

41 M. Itagaki, K. Hoshino, Y. Nakano, I. Shitanda and K. Watanabe, *Journal of Power Sources*, 2010, **195**, 6905.